H.A. FAYYADH

Department of Medical Physics, College of Applied Science, University of Fallujah
(Iraq)

FIRST-PRINCIPLES INVESTIGATION OF CONCENTRATION EFFECTS ON THE ELECTRONIC AND VIBRATIONAL PROPERTIES OF A BORON ALUMINUM PHOSPHIDE ALLOY WITH WURTZOID NANOSTRUCTURE

UDC 539

*The vibrational and electronic properties of the binary wurtzoids Al_7P_7 and B_7P_7 and the ternary one $B_xAl_{7-x}P_7$ have been investigated by the use of the approximation of the Density Functional Theory (DFT). By varying the concentration x, we carried out the calculations and various simulations of the bond lengths, energy gap, density of states, force constants, reduced masses, and infrared and Raman spectra. The geometric nanostructure of $B_xAl_{7-x}P_7$ wurtzoid has been analyzed using the Gauss view 05 program. As the concentration of B increases, the energy gap widens, indicating that the estimations are consistent with the experimental longitudinal optical measurements. We utilize the theoretical ab initio technique to mimic the properties and nanostructures of $B_xAl_{7-x}P_7$ wurtzoid using DFT B3LYP with the 6-311-G** basis sets and the GGA calculations with all electrons.*

K e y w o r d s: $B_xAl_{1-x}P_7$ wurtzoid, infrared and raman spectra, nanoscale.

1. Introduction

The important physical properties of semiconductor III-phosphides, namely, the low densities, high thermal conductivity levels, low dielectric constant, and wide bandgap, have sparked a lot of interest [1–7], owing to their extensive applicability in electronic and optoelectronic devices. BP possesses more sufficient covalent properties as compared with other III–V compounds, according to Bachir Bouhafs *et al.* [6], hinting that it can be employed in refractories. AlP is critical in the development and fabrication of transferred-electron devices, notably in the infrared photodetectors, because it is the III–V semiconductor with the largest indirect energy gap [7]. In the literature, there are numerous studies on III–III-phosphides ternary mixed alloy types. O. Nemiri *et al.* have carried out the research on electronic, thermodynamic, structural, and thermal characteristics of $InAs_xP_{1-x}$ alloys with the use of the full-potential linearized augmented plane wave (FP-LAPW) technique [8]. Bentouaf *et al.* used the full-potential linear muffin-tin orbital FP-LMTO technique to examine the electronic, optical, structural, and thermodynamic characteristics of $Al_xIn_{1-x}P$ and $AlAs_{1-x}P_x$ [9]. Lakel *et al.* [10] and Ma *et al.* [11] have investigated the electronic, mechanical, and optical characteristics of BAlP alloys. The latest researches by M.N. Rasul *et al.* and D. Hoat *et al.* [12, 13] have focused on the structural, optical, and electronic features of $B_{1-x}In_xP$ and $Ga_{1-x}B_xP$. Only the ternary compounds have direct band gap, while the BP compounds have indirect bandgap, according to the research by M.N. Rasul *et al.* [12], and III–III-phosphides ternary mixed alloys have been considered as important materials for optoelectronics, photoelectrics, and solar cell applica-

tions. The geometrical, electronic, and spectroscopic features of $B_xAl_{7-x}P_7$ as wurtzoid have been investigated in this paper using ab initio methods involving DFT.

2. Methods and Methodology

The importance of theoretical investigations of the properties of solids cannot be overstated. The determination of the energy bands or the calculation of the electron energy levels in the solids has been considered as a primary theoretical problem in the solid-state physics. Quantum mechanics methods were used for solving this challenge, by accounting for the motion and interactions of the electrons in the materials. In addition, quantum mechanics has been developed in order to provide a comprehensive explanation of atoms, particularly, light spectra that had been emitted by diverse species of atoms. The quantum theory of atoms has been developed in order to explain the reason for why the electrons have remained on orbitas that couldn't be described by Newton's laws of motion or Maxwell's conventional electromagnetic equations [14]. The present method uses, for all of the electrons, DFT B3LYP (3 parameters, Lee–Yang–Parr, Becke) with the valance triple-zeta 6-311-G** basis sets and GGA (i.e., generalized gradient approximations) calculations for the description of the properties and nanostructures of $B_xAl_{7-x}P_7$ wurtzoid utilizing the theoretical ab intio techniques. When employing B3LYP 6-311G**, vibrational frequency values must be adjusted with the use of 0.967 scale factors [15–17]. The Gauss view 05 program [18] and the Gaussian 09 software [19] were used to do all calculations. This work also investigates the molecular nanoscale limit regarding $B_xAl_{7-x}P_7$ as a concentration function. The researchers employed Gaussian 09 for constructing wurtzoid molecules at nanoscale limits that could be in material's wurtzite phase structure ($a \neq bc$) [20]. The Al_7P_7, $B_2Al_5P_7$, and B_7P_7 structures have been considered at nanoscale, as shown in Fig 1.

3. Results and Discussion

Following the geometric optimization, Fig. 2, *a, b*, and *c* illustrates the density of states of the ternary $B_2Al_5P_7$ wurtzoid and the binary (B_7P_7, Al_7P_7) wurtzoid as a function of their level of energy. As

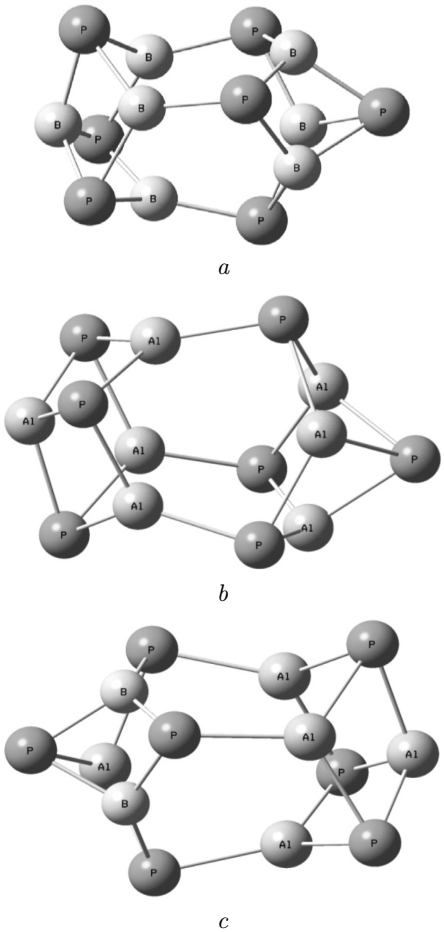

Fig. 1. Geometry of B_7P_7 (*a*), Al_7P_7 (*b*), $B_2Al_5P_7$ (*c*) wurtzoid nanotubes structure following the optimization

concentration of B rises, so does the density of states. The energy bandgap between low and high occupied molecular orbitals (V.B & C.B) of ternary wurtzoids (V.B & C.B) has been discovered to be tunable and variable around experimental values for Al_7P_7 and B_7P_7 in the range of 2.1 eV to 2.5 eV.

The present study is a research of the variation in the $B_xAl_{7-x}P_7$ wurtzoid concentration (x) as an energy gap function. It is found that if the B concentration grows, the magnitudes of energy gaps increase, as shown in Fig. 3. Energy levels have been limited to probable small-scale wells. In the case where the crystal becomes narrower, the bandgap rises, resulting in a greater energy gap as compared to the bulk [21, 22]. Due to the quantization confinement, energy gaps at nanoscale are rising [10, 11]. As a result, the

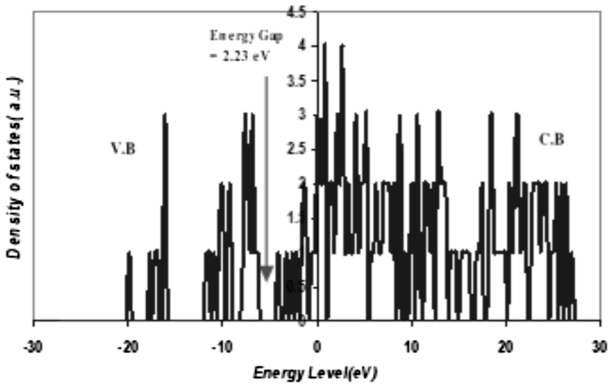

a

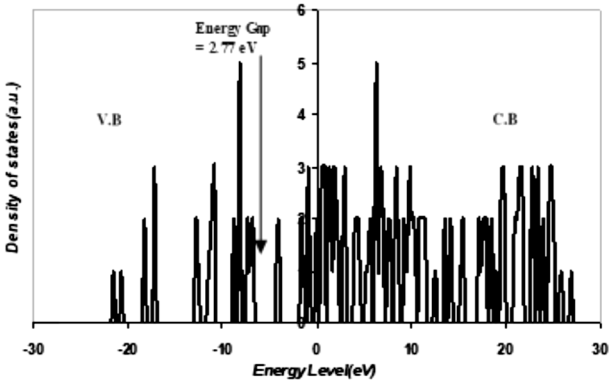

b

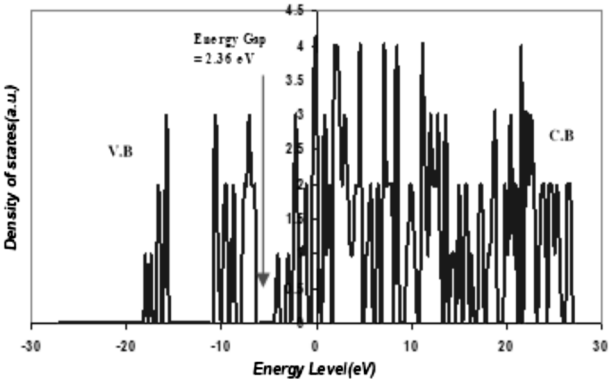

c

Fig. 2. $B_2Al_5P_7$ wurtzoid state density as a function of energy levels (*a*); B_7P_7 wurtzoid state density as a function of levels of the energy (*b*); Al_7P_7 wurtzoid state density as energy levels' function (*c*)

energy gaps in $B_2Al_5P_7$ from theoretical calculations are 2.1–2.7 eV.

Figure 4 depicts the bond length distribution density in the $B_2Al_5P_7$ wurtzoid, as compared with

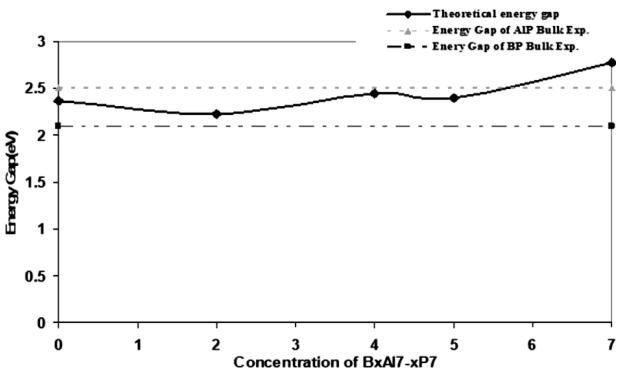

Fig. 3. $B_xAl_{7-x}P_7$ energy gaps are given as functions of the concentrations of B, Al, and P atoms and compared to experimental data

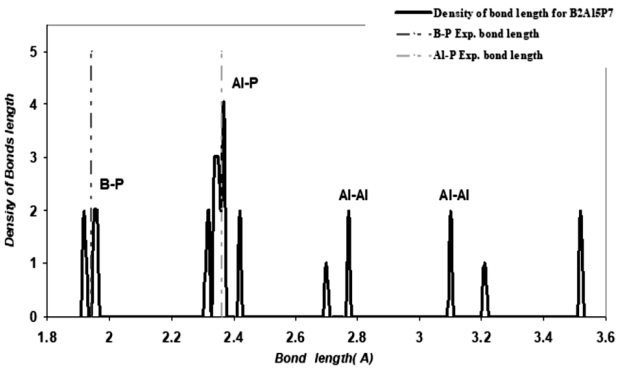

Fig. 4. Density of the $B_2Al_5P_7$ wurtzoid bonds as a function of the length of the bond (comparison to the bulk experimental data for the AlP and BP is presented)

the experimental bond values. Two available types of bonds are Al–P and B–P [23, 24]. The strongest bond is B–P one, followed by the Al–P bond. The bond length decreases with increasing the size of the molecule. The bond values match those discovered in experiments. In addition, the experimental values for the aforementioned bonds were 2.36 and 1.96 Å [23, 24].

Longitudinal optical (LO) vibrational modes of the $B_2Al_5P_7$ wurtzoid are represented as functions of the B concentration (x) in Fig. 5, *a, b*, and *c*. The nanoscale effect is that the frequency of the LO mode value is decreased [25]. Furthermore, the bare case has higher frequencies due to dangling bonds from the surface. The effect of a dangling bond is to increase the steady force. Figure 5 shows variations of Al_7P_7, B_7P_7, and $B_2Al_5P_7$ wurtzoid vi-

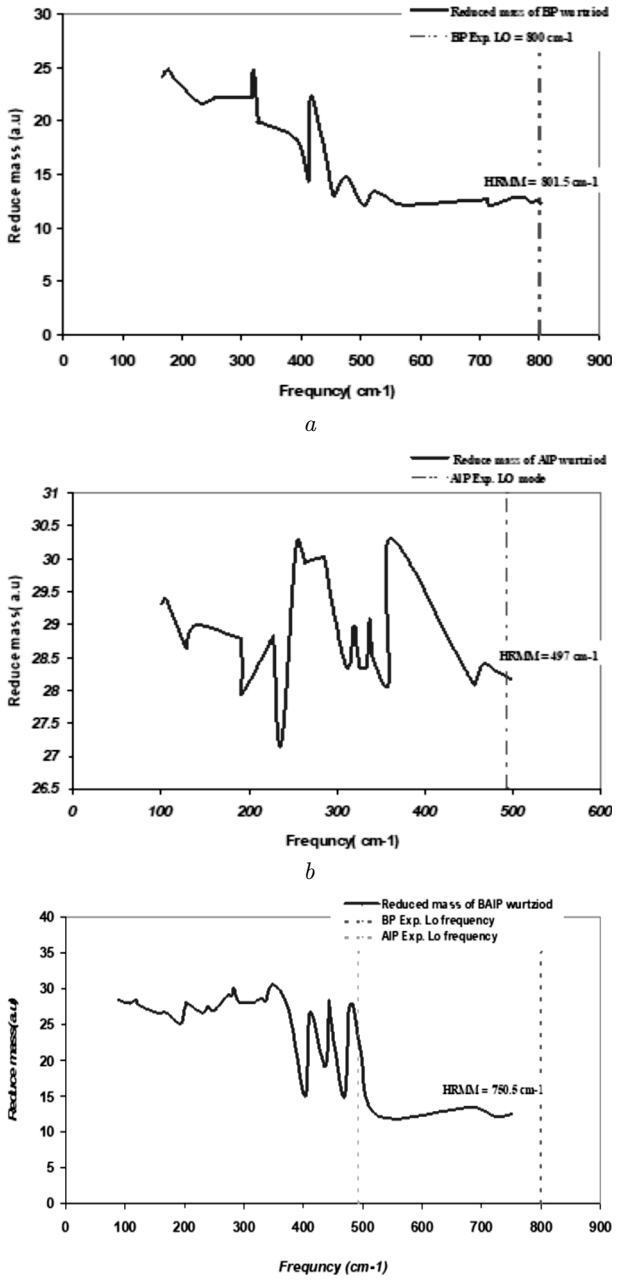

Fig. 5. Variations of B_7P_7, Al_7P_7, $B_2Al_5P_7$ wurtzoid vibrational reduced masses as functions of the frequency. The experimental LO vibration mode of the AlP and BP as shown in [27, 28] (*a, b*) and (*c*)

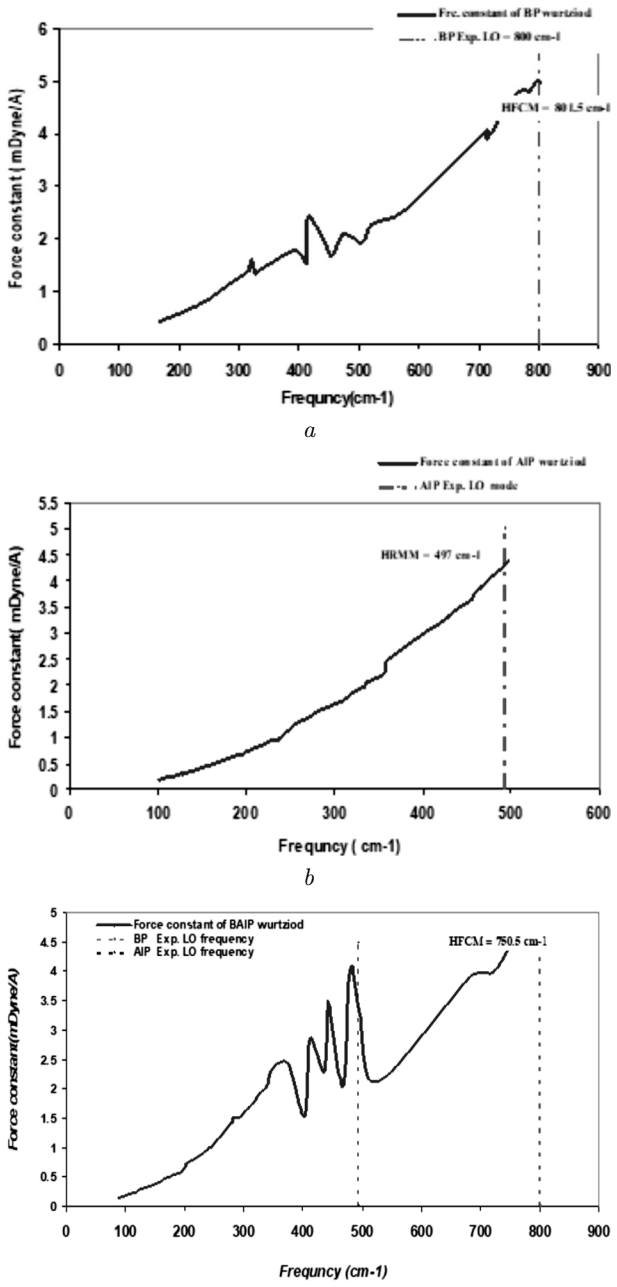

Fig. 6. Variations of B_7P_7,Al_7P_7, $B_2Al_5P_7$ wurtzoid vibration force constants as functions of the frequency. Experimental LO vibrational mode of AlP and BP (*a, b*, and *c*)

brational decreased mass drop as a frequency function. Figure 5, *a* shows that the highest reduced mass mode (HRMM) for B_7P_7 (wurtziod) equals 801.50 cm^{-1}, as compared to the bulk experimental LO mode (800 cm^{-1}) [26]. Figure 5, *b*, on the other hand, indicates that the HRMM for Al_7P_7 (wurtziod) equals 497 cm^{-1}, as compared to the bulk exper-

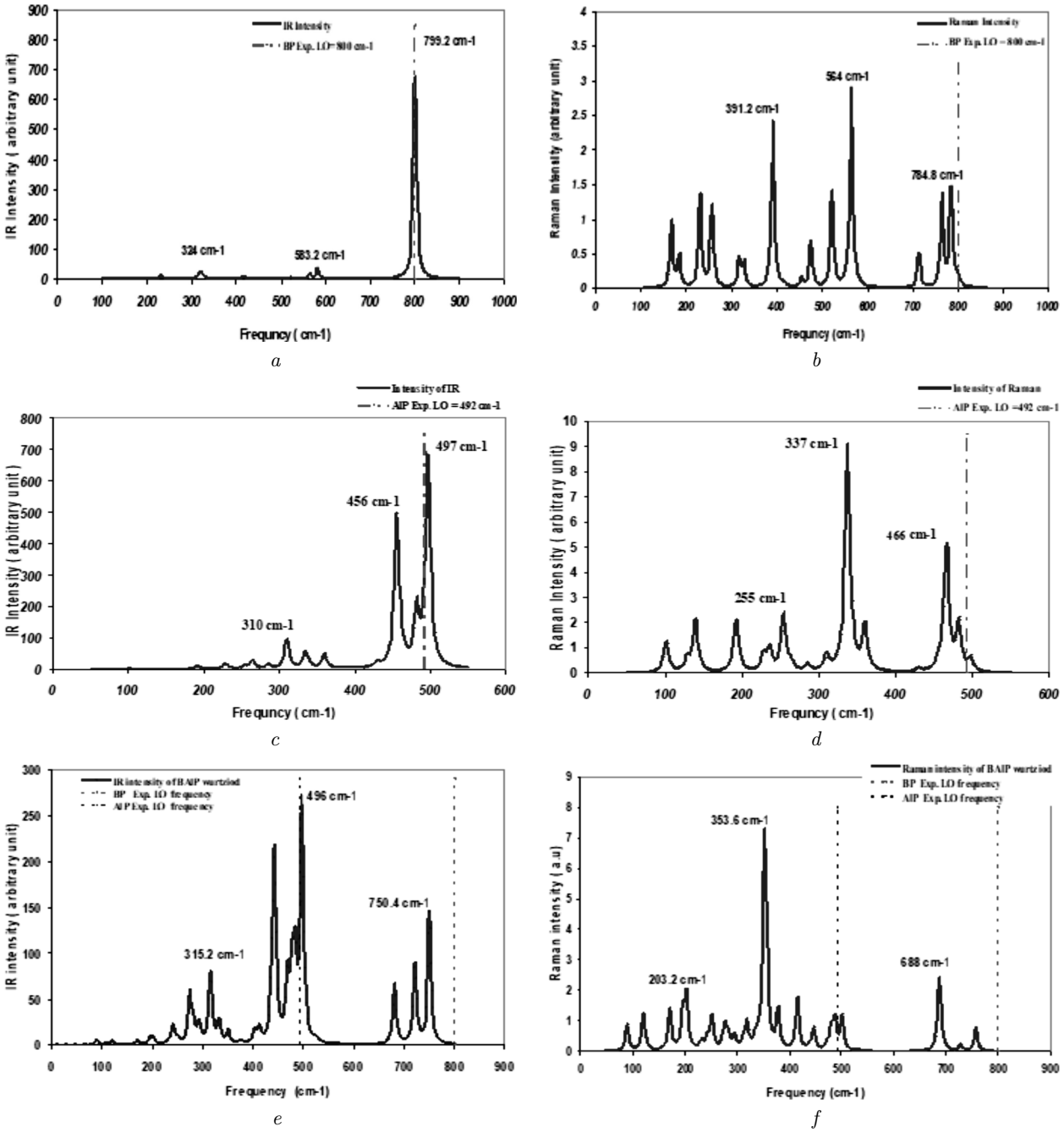

Fig. 7. Infrared and Raman spectra for the wurtzoid as a frequency function. Infrared spectrum of the B_7P_7 Wurtzoid (*a*), Raman spectrum of the B_7P_7 Wurtzoid (*b*), infrared spectrum of the Al_7P_7 Wurtzoid (*c*), Raman spectrum of the Al_7P_7 Wurtzoid (*d*). Infrared spectrum of $B_2Al_5P_7$ Wurtzoid (*e*), Raman spectrum of the $B_2Al_5P_7$ Wurtzoid (*f*)

imental LO mode (492 cm^{-1}). Lastly, in Fig. 5, *c*, the HRMM for $B_2Al_5P_7$ (wurtziod) is equivalent to 750.5 cm^{-1}. Since their atoms are not connected to other atoms, the bare molecules have a broad reduced mass value. According to the following equation, collections of heavy atoms vibrate initially and

have the lowest values of frequencies [27–30]:

$$\nu = \frac{1}{2\pi}\sqrt{\frac{k}{\mu}}, \tag{1}$$

where μ represents the reduced mass, and k is the force constant.

Figure 6, *a, b* and *c* shows the Al_7P_7, B_7P_7, and $B_2Al_5P_7$ wurtzoid vibration force constants as functions of the frequency, revealing that the values of the frequency are directly proportional to the constant of force, whereas the values in the present study correspond to the highest value of the LO mode. The compound's dangling bonds have the effect of increasing the frequencies, which causes the force constant to rise in response.

Figure 7, *a* shows infrared intensity spectrum for the B_7P_7 wurtziod that shows 2 regions: the first one with a central peak at 324 cm^{-1} and the second one with a central peak at 799.2 cm^{-1}. They are close to the experimental value of LO, which equals 800 cm^{-1} (24.00 THz) [27]. In contrast, Fig. 7, *b* depicts a Raman spectrum with a very low intensity in those 2 bands.

Figure 7, *c* shows the infrared spectrum for the Al_7P_7 wurtzoid that has diverse bands at 2 regions of 310 cm^{-1}& 497.2 cm^{-1} that is close to the experimental value of LO = 492 cm^{-1} [28]. In addition, Raman spectra have been obtained at 466 cm^{-1} with a very low intensity in such bands as shown in Fig. 7, *d.* The Raman and infrared spectra of $B_2Al_5P_7$ wurtzoid are shown in Fig. 7, *e, f.* Hence, the theoretical value agrees with the observed value. The results of this study correspond to those for the ternary compound wurtzoid.

4. Conclusion

This research looked at the vibrational and electronic features of binary BP and AlP compounds, along with their ternary mixed $B_xAl_{7-x}P_7$ wurtzoid materials, using the DFT approximation. The experimental gap that is associated with the energy value regarding the binary bulk B_7P_7 and Al_7P_7 is found to be closer to theoretical values of the BP, as well as AlP wurtzoid, while the gap related to energy values of the ternary BAlP Wurtzoid has been associated directly to the increase of the B concentration. The greatest peaks of structural parameters such as bond lengths have a value distribution that is closer to ideal values of the bulk of these parameters. The vibration frequency effects on the reduced masses and force constants have been extremely close to their optimal bulk values. The calculations show the frequency dependence for the Al_7P_7, B_7P_7, and $B_2Al_5P_7$ wurtzoid vibration force constants, revealing that the values of the frequency are directly proportional to the constant of force, whereas values in the present study correspond to the highest value of the LO mode. Furthermore, it is discovered that the IR and Raman spectral intensities accord with regard for experimental data.

1. R.W.G. Wyckoff. *Crystal Structures. 2nd Edition* (Krieger, 1986).
2. O. Madelung. *Semiconductors: Data Handbook* (Springer, 2004) [ISBN: 978-3-642-18865-7].
3. I. Vurgaftman, J.R. Meyer, L.R. Ram-Mohan. Band parameters for III–V compound semiconductors and their alloys. *J. Appl. Phys.* **89**, 5815 (2001).
4. R.M. Wentzcovitch, M.L. Cohen. Theory of structural and electronic properties of BAs. *J. Phys. C Solid State Phys.* **19**, 6791 (1986).
5. E. Schroten, A. Geossens, J. Schoonman. Photo- and electro reflectance of cubic boron phosphide. *J. Appl. Phys.* **83** (3), 1660 (1998).
6. B. Bouhafs, H. Aourag, M. Cartier. Trends in band-gap pressure coefficients in boron compounds BP, BAs, and BSb. *J. Phys. Condens. Matter.* **12**, 5655 (2000).
7. W.T. Masselink, A.A. Ketterson, J.S. Gedymin, J. Klem, C.K. Peng, W.F. Kopp, H. Morkoc, K.R. Gleason. Characterization of InGaAs/AlGaAs pseudomorphic modulation-doped field-effect transistors. *IEEE Trans. on Electron Devices* **33**, 564 (1986).
8. O. Nemiri, S. Ghemid, Z. Chouahda, H. Meradji, F. El Haj Hassan. Structural, electronic, thermodynamic and thermal properties of zinc blende InP, InAs and their $InAs_x P_{1-x}$ ternary alloys via first principles calculations. *Int. J. Mod. Phys. B* **27** (25), 1350166 (2013).
9. A. Bentouaf, M. Ameri, R. Mebsout, D. Hachemane, Theoretical study of structural, electronic, optical and thermodynamic properties of AlP, InP and AlAs compounds. *J. Optoelectron. Adv. Mater.* **7** (9–10), 659 (2013).
10. S. Lakel, F. Okbi, H. Meradji. Optical and electronic properties of $B_xAl_{1-x}P$ alloys: A first principles study. *Optik* **127**, 3755 (2016).
11. Huihui Ma, Junqin Zhang, Bin Zhao, Qun Wei, Yintang Yang. First-principles study on mechanical and elastic properties of $B_xAl_{1-x}P$ alloys. *AIP Advances* **7**, 065007 (2017).
12. M.N. Rasul, A. Anam, M. Atif Sattar, A. Manzoor, A. Hussain. DFT based structural, electronic and optical properties of $B_{1-x}In_xP$ (x = 0.0, 0.25, 0.5, 0.75, 1.0) compounds:

PBE-GGA vs. mBJ-approaches. *Chin. J. Phys.* **56**, 2659 (2018).
13. D.M. Hoat, J.F. Rivas Silva, A. Mendez Blas. First principles study on structural, electronic and optical properties of $Ga_{1-x}B_xP$ ternary alloys ($x = 0$, 0.25, 0.5, 0.75 and 1). *Phys. Lett.* **382**, 19421949 (2018).
14. V.A. Fock. *Fundamental of Quantum Mechanics* (Mir publishers, 1986).
15. R.D. Johnson III. *NIST Computational Chemistry Comparison and Benchmark Database* (Reference Database Number 101 Release, 1999).
16. M.T. Hussein, T.A. Fayad, M.A. Abdulsattar. Concentration effects on electronic and spectroscopic properties of ZnCdS wurtzoids: A Density functional theory study. *Chalcogenide Lett.* **16** (11), 557 (2019).
17. M.T. Hussein, H.A. Thjeel. Study of geometrical and electronic properties of ZnS wurtzoids via DFT. *Chalcogenide Lett.* **15** (10), 523 (2018).
18. A. Frisch, H.P. Hratchian, R.D. Dennington, II, T.A. Keith, J. Millam, A.B. Nielsen, A.J. Holder, J. Hiscocks. *GaussView Version 5.0* (Gaussian Inc., 2009).
19. M.J. Frisch, G.W. Trucks, H.B. Schlegel, G.E. Scuseria, M.A. Robb, J.R. Cheeseman, G. Scalmani, V. Barone, B. Mennucci, G.A. Petersson, H. Nakatsuji, M. Caricato, X. Li, H.P. Hratchian, A.F. Izmaylov *et al. Gaussian 09* (Gaussian Inc., 2009).
20. V.P. Kumar, A.Y. Sharma, D.K. Sharma, D.K. Dwivedi. Effect of sintering aid ($CdCl_2$) on the optical and structural properties of CdZnS screen-printed film. *Opt. Int. J. Light Electron. Optics* **125**, 1209 (2014).
21. T.P. Sharma, D. Patidar, N.S. Saxena, K. Sharma. Measurement of structural and optical band gaps of $Cd_{1-x}Zn_x$ ($x = 4$ and 6) nanomaterials. *Indian J. Pure Appl. Phys.* **44** (2), 125 (2006).
22. M.A. Mahdi, S.K. Al-Ani. Optical characterization of chemical bath deposition $Cd_{1-x}Zn_xS$ thin films. *Int. J. Nanoelectron. Mater.* **5**, 11 (2012).
23. Saif Ullah, Pablo A. Denis,and Fernando Sato. Hydrogenation and fluorination of 2d boron phosphide and boron arsenide: A density functional theory investigation., *ACS Omega* **3**, 16416 (2018).
24. K.J. Chang, S. Froyen, M.L. Cohen. Electronic band structures for zinc-blende and wurtzite CdS. *Phys. Rev. B* **28**, 4736 (1983).
25. S. Farid, M.A. Stroscio, M. Dutta. Multiphonon Raman scattering and photoluminescence studies of CdS nanocrystals grown by thermal evaporation. *Super Lattices and Microstructures* **115**, 204 (2018).
26. O. Brafman, G. Lengyel, S.S. Mitra. Raman spectra of AℓN, cubic BN and BP. *SolLd State Communications* **6**, 523 (1968).
27. H.W. Leite Alves, K. Kunc. Lattice dynamics of boron phosphide. *J. Phys.: Condens. Marter.* **4**, 6603 (1992).
28. S.Q. Wang, H.Q. Ye. Ab initio investigation of the pressure dependences of phonon and dielectric properties for III–V semiconductors. *J. Phys.: Condens. Matter.* **17**, 4475 (2005).
29. H.A. Fayyadh. Stability, Structural and Electronic properties of indium phosphide wurtzite-diamantane molecules and nanocrystals: A density functional theory study. *J. Nano Research* **69**, 1 (2021).
30. M.M. Habib, M.T. Hussein. Study the electronic and spectroscopic properties of $Al_xB_{7-x}N_7$ Wurtzoids as a function of size and concentration using density functional theory. *Materials Today: Proceedings* **42**, 2353 (2021).

Received 26.07.22

Х.А. Файядх

ДОСЛІДЖЕННЯ НА БАЗІ ПЕРШИХ ПРИНЦИПІВ ВПЛИВУ КОНЦЕНТРАЦІЇ НА ЕЛЕКТРОННІ ТА ВІБРАЦІЙНІ ВЛАСТИВОСТІ БОР–АЛЮМІНОФОСФІДНОГО СПЛАВУ З ВУРЦОЇДНОЮ НАНОСТРУКТУРОЮ

Розглядаються вібраційні та електронні властивості бінарних Al_7P_7 і B_7P_7 та потрійного $B_xAl_{7-x}P_7$ вурцоїдів з використанням теорії функціонала густини (ТФГ). Для різних концентрацій x виконано розрахунки і моделювання довжин зв'язків, енергетичної щілини, густини станів, силових констант, редукованих мас та інфрачервоних і раманівських спектрів. Використовуючи програму Gauss view 05, ми проаналізували геометричну наноструктуру сполуки $B_xAl_{7-x}P_7$. Енергетична щілина стає ширшою, коли концентрація бору зростає, що узгоджується з експериментальними даними. У розрахунках для всіх електронів використано метод B3LYP ТФГ у базисі 6-311-G** в узагальненому градієнтному наближенні.

Ключові слова: $B_xAl_{1-x}P_7$ вурцоїд, інфрачервоний і раманівський спектри, наномасштаб.